

Dynamical properties of the hypercell spin glass model

P. M. Gleiser F. A. Tamarit *

Facultad de Matemática, Astronomía y Física

Universidad Nacional de Córdoba

Ciudad Universitaria, 5000 Córdoba, Argentina

(April 14, 2017)

Abstract

The spreading of damage technique is used to study the sensibility to initial conditions in a heat bath Monte Carlo simulation of the spin glass hypercubic cell model. Since the hypercubic cell in dimension 2D and the hypercubic lattice in dimension D resemble each other closely at finite dimensions and both converge to mean field when dimension goes to infinity, it allows us to study the effect of dimensionality on the dynamical behavior of spin glasses.

Typeset using REVTeX

*E-mail: pgleiser@fis.uncor.edu and tamarit@fis.uncor.edu

I. INTRODUCTION

The spin glass theory has been one of the most difficult problems treated by statistical mechanics during the last two decades. Despite its value in the field of solid state physics, its study has also contributed to develop new techniques which now apply to a wide range of fields, such as optimization problems, neural networks, and other complex systems [1].

The first microscopic approach to spin glasses is due to Edwards and Anderson (EA) [2], whose model basically consists on a Ising system with random positive and negative exchange couplings. Until now only its mean field version, known as the Sherrington Kirkpatrick model (SK) [3] has been exactly solved, but unfortunately its solution requires the sophisticated replica trick. Under such limitations, Monte Carlo numerical simulations have become one of the most applied techniques in the field. At the same time, it is not clear at the moment whether one should expect that the spin glass phase of the mean field SK model resembles the behavior of the spin glass phase of the low dimension EA model.

For many years there has been great controversy on whether the spin glass transition is either of thermodynamical or dynamical nature. However numerical simulations [4] and phenomenological scaling arguments at zero temperature [5] strongly suggest the existence of a true thermodynamical phase transition. From a dynamical point of view, a very careful numerical study of the time decay of the auto-correlation function $q(t)$ has shown that the system displays three different dynamical regimes: above the Curie point T_c of the nonrandom Ising model, the auto-correlation decays exponentially; between T_c and the spin glass temperature T_g the auto-correlation function has a stretched exponential behavior with temperature dependent exponents; finally, in the spin glass phase only power law decay is observed at all times scales.

Since the SK model can be understood as the infinite dimension version of the EA model, it is desirable to be able to study the effects of dimensionality both in the static and dynamical properties of the system, even if such analysis should be limited to numerical considerations. In 1992 Parisi, Ritort and Rubí [6] introduced the *hypercubic cell model*

which allows a very efficient treatment of high dimensional models, at least when compared with hypercubic lattice models. It consists of a unique cubic cell of dimension D with an Ising spin variable associated to each of its 2^D corners. Despite its simplicity and unrealistic features, one expects that its behavior for dimension $2D$, resembles, at least qualitatively, that observed in a D dimensional hypercubic lattice, since both share the same connectivity D . Even more, for $D \rightarrow \infty$ the hypercell model recovers the mean field SK model.

This approach has been used in the last few years to analyze both dynamical and statical consequences of dimensionality in the spin glass phase of different models [6–9]. In this work we apply the damage spreading method to the hypercell Ising spin glass model simulated with a heat bath Monte Carlo dynamics. This technique basically consists in measuring the time evolution of the Hamming distance between two initially different configurations submitted to the same thermal noise, i.e, updated with the same random number sequence. The dependence of the damage and other related quantities on temperature, time, initial conditions and other relevant parameters leads to a dynamical phase diagram of the model.

In general, this phase diagram strongly depends on the Monte Carlo dynamics used in the numerical simulation. In particular, for the bi and three-dimensional Ising ferromagnet one finds that the dynamical transition coincides with the static one when the system is submitted to heat bath dynamics, while the opposite occurs when submitted to Glauber dynamics. When more complex systems are analyzed with heat bath dynamics, more than two dynamical phases are usually found, where only a few of them are correlated with thermodynamical phases (see [11] and references therein). In particular, for spin glasses in three and four dimensions [10], three different dynamical regimes were obtained, as occurred when the auto-correlation was analyzed. For low temperatures, the final damage is non null and its value depends on the initial Hamming distance. For intermediate temperatures, the damage still spreads but its final value is independent on the initial damage. Finally, for high temperature the final damage is always zero. While the lower dynamical transition temperature seems to agree with the equilibrium one (T_g) separating the spin glass and the paramagnetic phases, the upper transition temperature seems to be consistent with the

temperature below which the stretched exponential relaxation emerges (T_c). Surprisingly, a similar behavior was reported for the two dimensional spin glass model, which does not present a non zero temperature spin glass phase. Nevertheless, despite some numerical evidence, it is not clear whether these three regimes found with damage spreading are related to those observed through the temporal behavior of the auto-correlation function. On the other hand, when the SK model was studied only a two phases structure was found, in good agreement with the thermodynamical diagram.

This paper is organized as follows. In section 2 we introduce in more detail the hypercell model and describe the spreading of damage technique. In section 3 we present the results for different dimensions. Finally, in section 4 we discuss the main conclusions of the paper.

II. THE MODEL AND THE METHOD

The model consists of a single hypercubic cell in dimension D with an Ising spin variable $S_i = \pm 1$ associated to each of its 2^D corners. Each spin interacts with its D nearest neighbours through the Hamiltonian

$$H = - \sum_{\langle ij \rangle} J_{ij} S_i S_j, \quad (1)$$

where $\langle ij \rangle$ denotes nearest neighbours and the J_{ij} are chosen accordingly to the following probability distribution:

$$P_J(J_{ij}) = \frac{1}{2} \delta(J_{ij} - J) + \frac{1}{2} \delta(J_{ij} + J). \quad (2)$$

Here we have taken $J = 1/D^{1/2}$ to normalize extensive quantities.

The method consists on simulating the time evolution of the system through a heat bath Monte Carlo process. The spins are sequentially updated with the following rule:

$$S_i(t+1) = \begin{cases} +1 & \text{with probability } \frac{1}{2}[1 + \tanh(h_i(t))] \\ -1 & \text{with probability } \frac{1}{2}[1 - \tanh(h_i(t))] \end{cases} \quad (3)$$

where $h_i = \sum_{i \neq j}^N J_{ij} S_i(t)$ is the local field in site i at time t .

For a given disorder configuration $\{J_{ij}\}$ we choose two different initial states $\{S_i^A\}$ and $\{S_i^B\}$ and let both evolve with the same thermal noise, i.e., by using the same random sequence. We then measure the time evolution of the Hamming distance or *damage* between them, defined as

$$dh(t) = \frac{1}{4N} \sum_i^N (S_i^A(t) - S_i^B(t))^2. \quad (4)$$

For each temperature we calculate the time average of the damage $\overline{\langle dh \rangle}$ over 10000 Monte Carlo Steps (MCS), defined by:

$$\overline{\langle dh \rangle} = \frac{\sum_t \langle dh \rangle(t) P(t)}{\sum_t P(t)}. \quad (5)$$

Here $P(t)$ is the probability that the two replicas do not become identical at time t [10]. Note that, since we use the same random sequence for updating both replicas, if at any time t they become identical (i.e., they meet in the phase space), they will continue identical for all subsequent times.

This procedure was repeated M times (M depending on D and T) in order to obtain a configurational average $\langle dh \rangle$ of the damage over different coupling constants, initial conditions and random number sequences.

In the next section we will study the influence of the dimensionality D and the initial damage between the two replicas $dh(0)$ in the long time behavior of the Hamming distance. This will allow us to characterize different dynamical behaviors as a function of the temperature of the system and analyze their possible relationships with the thermodynamical phases.

III. RESULTS

We start this section by describing the behavior of the model for dimension $D = 8$. In Fig. 1 we show the Hamming distance as a function of temperature for three different initial damages, namely, $dh(0) = 0.1, 0.5$ and 1 .

Observe that the system displays three different dynamical regimes:

- a) for low temperatures ($T < T_1^8$) we observe that $\langle dh \rangle$ is non null and its value depends on the initial damage (it increases as the initial damage increases);
- b) for intermediate temperatures ($T_1^8 < T < T_2^8$) the system is characterized by a single value of $\langle dh \rangle$ independent of the initial damage;
- c) for high temperatures ($T > T_2^8$) the Hamming distance $\langle dh \rangle$ is always zero.

This behavior is similar to the one observed by Derrida and Weisbuch [10] in the three-dimensional Edwards-Anderson model and differs from that observed on the Sherrington-Kirkpatrick model, as described in the introduction. As we will show soon, the same qualitative behavior was also observed for $D = 6, 10$ and 15 .

Next we characterize each phase by the temporal behavior of both P and $\langle dh \rangle$. In Fig. 2 we show the behavior of $P(t)$ and $\langle dh \rangle(t)$ for $T = 0.53$ (the low temperature phase), with $dh(0) = 1$.

After suffering an exponential decay to a value close to 0.5 (a similar behavior was observed by Arcangelis *et al.* [12] for the EA model) the Hamming distance $\langle dh \rangle(t)$ grows slowly, while $P(t)$ decays slowly too. In Fig. 3 we show the same results in a double logarithmic plot, from which follows that, after an initial transient of about 1000 MCS both quantities vary with a power law behavior $P(t) \approx t^{-\delta}$ (with $\delta \approx 0.258$) and $\langle dh \rangle(t) \approx t^{-\gamma}$ (with $\gamma \approx 0.047$). We have also found that these exponents depend on the temperature of the system, although a more careful analysis of such dependence should be done with better statistics and for different temperatures in order to confirm these results.

This behavior can be understood in terms of the phase space structure of the system. If, as happens in the SK model, the phase space has valleys separated by a wide distribution of Hamming distances, then the replicas that are closer to each other become identical faster than those that are further apart. As time goes on, $\langle dh \rangle$ takes into account only those replicas that are far apart and, as a consequence, it grows. This indicates that bigger energy

barriers separate valleys that are further apart. Since we are working with small systems, $N = 256$, these barriers can be crossed for long times as the ones we considered ($t = 10000$).

Next we make a similar study in the intermediate phase. In Fig. 4 we plot the curve $\ln(-\ln P(t))$ vs. $\ln t$ for $T = 1.41$, which, for a wide range of values of t , can be very well fitted by a linear function indicating a stretched exponential decay of $P(t)$. The Hamming distance presents a different behavior, since it remains constant as time flows and $P(t)$ decays. For long times $\langle dh \rangle$ displays big fluctuations, which appear as a consequence of the poor statistics (note that only a small number of replicas have survived for such long times). These results accept three different interpretations:

- the system has a phase space structure with multiple valleys but all of them equidistant;
- the system has only two valleys, like a ferromagnet;
- the phase space is almost flat as a function of the free energy, so the two replicas wander through a phase space (represented by a hypercube of dimension 2^{2^D}) and do not find themselves due to its high dimensionality.

In the first two hypotheses, the faster decay of $P(t)$ indicates that the valleys are not mutually impenetrable. It is probable then that in this paramagnetic phase the system separates regions in phase space (valleys) that are accessible to each other.

Finally, in the high temperature phase ($T > T_2^6$) all the replicas become zero in a few MCS and both $P(t)$ and $\langle dh \rangle$ decays exponentially.

These results are very important since:

- $P(t)$ has a temporal behavior similar to the one found in [4], indicating the possibility of a close relationship between the phases found with spreading of damage and those studied through the auto-correlation function $q(t)$;
- they show that the hypercell model in dimension $D = 8$ is similar to the three and four dimensional EA model not only in its static properties (as studied by Parisi *et al.* [6]) *but also* in its dynamical behavior.

The same detailed study was performed for $D = 6$ and the same qualitative behavior was observed for all the quantities.

In dimension $D = 10$ a new dynamical behavior emerges. In considering the $\langle dh \rangle$ vs. T plot presented in Fig. 5, we see that the system basically displays the same three regimes found in $D = 8$. Nevertheless a more detailed analysis of the dependence of P and $\langle dh \rangle$ with time, showed in Fig. 6, reveals new features. Now both in the intermediate and the lower temperature phases $P(t)$ equals 1 for all considered times ($t < 10000$) while $\langle dh \rangle$ keeps a constant value (after an initial fast exponential decay). The only difference resides in the dependence on the initial damage shown in Fig. 5.

The difference between this phases can be better observed in Fig. 7 where we present the histograms of Hamming distances in $t = 100$ for $T = 0.35$ and $T = 1.92$ respectively, with initial damage $dh(0) = 1$. We verify that the low temperature phase still presents a wide distribution, indicating a complex structure as the one described by replica symmetry breaking. On the other hand, in the intermediate regime the distribution is narrow, indicating a behavior that corresponds to one of the three hipotesis made for the $D = 8$ case. It is worth mentioning that the histograms present the same qualitative behavior in all studied dimensions indicating a drastic change in the phase space structure at the critical temperature T_1 .

The same analysis has been done for $D = 15$ and in Fig. 8 we present $\langle dh \rangle$ vs. T with the three usual phases. The temporal analysis displays the same behavior in the different phases.

Finally, in table (IV) we present the values of the critical temperatures T_1^D and T_2^D obtained for the different dimensions studied in this paper.

Note that as D increases, T_1 seems to approach, as expected, the value 1, which corresponds to the critical static temperature of the Sherrington Kirkpatrick model. Unfortunately, as much as we know, the static critical temperatures of the spin glass-paramagnetic transition for finite D have never been studied, so, it is impossible to compare static and dynamical transition temperatures. If, as happens with all Ising like spin models studied in

the literature with heat bath dynamics, these temperatures coincide, we can then conclude that the convergence of this critical temperature T_1 is very slow. Concerning T_2 , it also increases, but higher dimensions should be considered in order to extrapolate the $D \rightarrow \infty$ behavior. It is important here to stress that, at least for $D = 15$, we have not found a dynamical behavior that resembles the one obtained in the study of the Sherrington Kirkpatrick model, namely, a two phase structure with the critical dynamical temperature in good agreement with the static one. In other words, for all the temperatures considered in this paper, we have shown that the system has a dynamical phase diagram similar to the one of the Edwards–Anderson model, i.e., we did not find an *upper critical dynamical dimension* above which the system displays a mean field behavior.

IV. CONCLUSIONS

In this work we have applied the damage spreading technique to the hypercell Isin spin glass model in order to study its dynamical behavior and the influence of dimensionality. As was stressed in the introduction, previous studies had found different dynamical phase diagrams for the EA and the SK model. While the former presented three different regimes (suggesting a correlation with the temporal decay of the autocorrelation function), the last one presented a unique phase transition at a temperature compatible with the spin glass–paramagnet static transition. Since the SK model is recovered as the $D \rightarrow \infty$ version of the EA model, we studied the effect of increasing the dimensionality in the dynamical behavior of the system in the hope of finding some critical dimension above which the system displays the mean field dynamical phase diagram.

The phase diagram, for all dimensions studied, presents a three phase structure similar to that obtained for the EA model with $D = 3$ and $D = 4$, namely, a low temperature phase that displays dependence with the initial damage, an intermediate phase where the damage spreads but its final value is independent of the initial damage and a high temperature phase where the damage decays exponentially to zero. While the lower critical dynamical

temperature seems to converge to SK static temperature, for the upper critical temperature we were not able to extrapolate its behavior (we are probably far from an asymptotic regime). This means that, at least for $D = 15$, we are still far from the SK regime. Further simulations with higher dimensions would be required but the computation time needed exceeds our numerical capacity.

When one considers the temporal behavior of the quantity $P(t)$ for different dimensions, some interesting conclusion can be extracted:

- There is a drastic change in the behavior of $P(t)$ for $D \leq 8$ and $D \geq 10$. In the former case, $P(t)$ displays a decay similar to that observed for the auto-correlation function in the EA model [4] characterizing three different phases: power law decay for $T < T_1^D$, stretched exponential decay for $T_1^D < T < T_2^D$ and exponential decay for $T > T_2^D$. In the last case ($D \geq 10$), $P(t)$ is constant and equals 1 in the low and intermediate temperature regimes and decays exponentially in the high temperature phase ($T > T_2^D$).
- The detailed analysis of the histograms of Hamming distances reveals that the low temperature phase is characterized by a wide distribution, as expected in a multi-valley phase diagram, for all the dimensions considered. This structure resembles, at least qualitatively, the one found in the SK model. On the other hand, in the intermediate phases we always found narrow distributions of the Hamming distances. Note that in this regime the final distance is always non zero independently of the initial damage. This is also true for vanishing small initial damages, meaning that in this phase the heat bath Monte Carlo dynamics is truly chaotic.

ACKNOWLEDGMENTS

We are gratefully acknowledged to D.A. Stariolo for fruitful discussions.

FIGURES

FIG. 1. $\langle dh \rangle$ vs Temperature for $D = 8$ and for three different initial damages: $dh(0) = 1$ (triangles), $dh(0) = 0.5$ (squares) and $dh(0) = 0.1$ (circles).

FIG. 2. Temporal behavior of $P(t)$ and $\langle dh \rangle(t)$ for $D = 8$ and $dh(0) = 1$. The average was calculated over 1000 different samples.

FIG. 3. $\langle dh \rangle$ and $P(t)$ as a function of t in a double logarithmic scale for $D = 8$ and $T = 0.52$ (in the low temperature phase).

FIG. 4. $\ln(-\ln \langle dh \rangle)$ and $\ln(-\ln P(t))$ for $D = 8$ and $T = 1.41$, (in the intermediate phase).

FIG. 5. $\langle dh \rangle$ vs Temperature for $D = 10$ and for three different initial damages: $dh(0) = 1$ (triangles), $dh(0) = 0.5$ (squares) and $dh(0) = 0.1$ (circles).

FIG. 6. $\langle dh \rangle$ vs. t for $D = 10$, $dh(0) = 1$ and for $T = 0.35$ (low temperature phase) and $T = 1.92$ (intermediate phase).

FIG. 7. Histogram of Hamming distances at $t = 100$ with $dh(0) = 1$. for $D = 10$ and a) $T = 0.35$ (in the low temperature phase) and b) $T = 1.92$ (in the intermediate phase).

FIG. 8. $\langle dh \rangle$ vs Temperature for $D = 15$ and for two different initial damages: $dh(0) = 1$ (circles), $dh(0) = 0.5$ (squares).

TABLES

D	T_1^D	T_2^D
6	0.65 ± 0.04	1.8 ± 0.2
8	0.66 ± 0.04	1.7 ± 0.1
10	0.74 ± 0.08	2.0 ± 0.1
15	0.79 ± 0.01	3.25 ± 0.05

REFERENCES

- [1] K.H. Fischer and J.A. Hertz, *Spin Glasses*, Cambridge University Press, Great Britain, 1993
- [2] S.F. Edwards and P.W. Anderson, *J. Phys.* **F 5**, 965 (1975)
- [3] D. Sherrington and S. Kirkpatrick, *Phys. Rev. Lett.* **35**, 1792 (1975)
- [4] Ogielski A.T. *Phys. Rev. Lett.* **54**, 928 (1985)
- [5] A.J. Bray and M.A. Moore *J. Phys C:Solid State Phys.***17** L463, L613 (1984)
A.J. Bray *Comment Cond. Mat. Phys.* **14** 21 (1988)
- [6] Parisi G.,Ritort F., Rubí J.M. (1991) *J.Phys.A:Math.Gen* **24** 5307
- [7] L. Cugliandolo and J. Kurchan, *J. Phys. A* **27**, 5749 (1994)
- [8] E. Marinari, G. Parisi and F. Ritort, *J. Phys. A***28**, 327 (1995)
- [9] D. Stariolo, preprint CONDMAT/9607132
- [10] Derrida B., Weisbuch G. (1987), *Europhys. Lett.* **4**, 657
- [11] L. da Silva, F.A. Tamarit and A.C.N. de Magalhães, *J. Phys. A* **30**, 2329 (1997)
- [12] De Arcangelis L. (1990), in *Correlations and Connectivity*, edited by Stanley H. E. and Ostrowsky N. (Kluver Acad. Publ.)

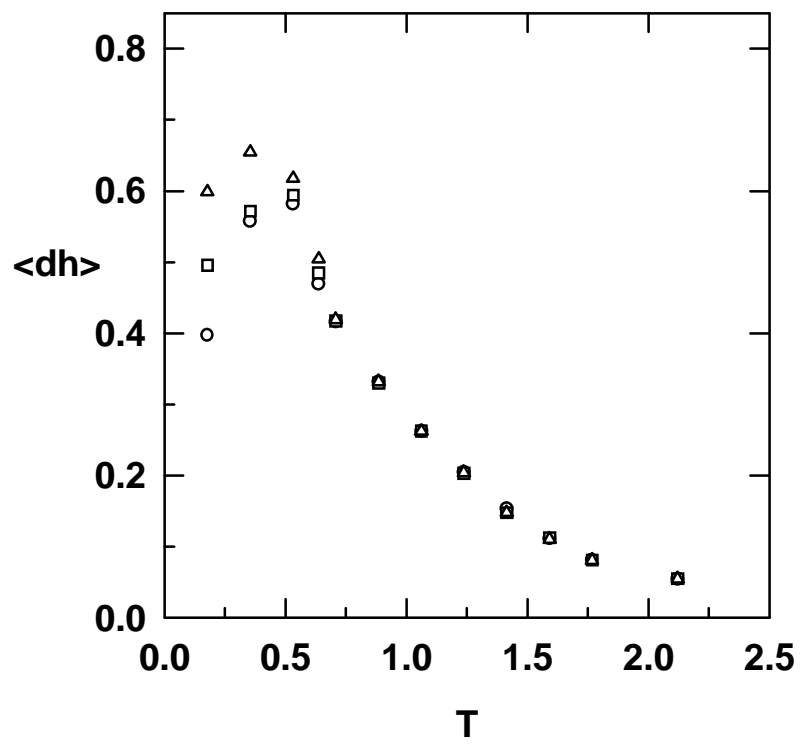


FIGURE 1

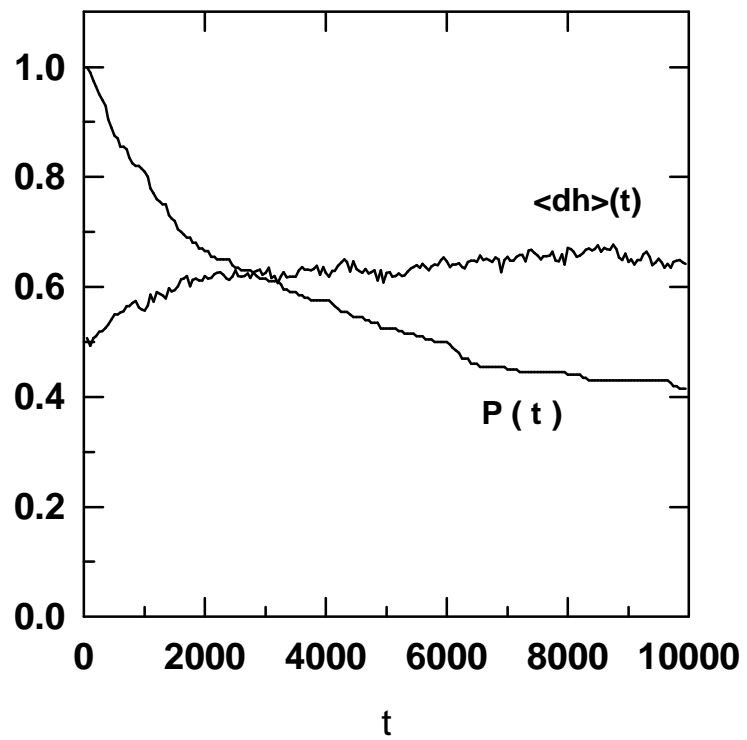


FIGURE 2

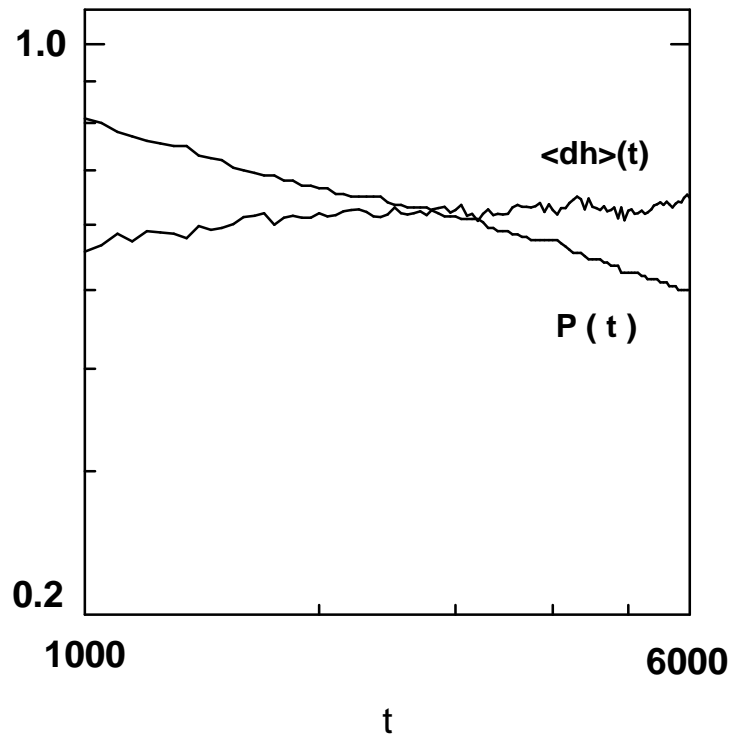


FIGURE 3

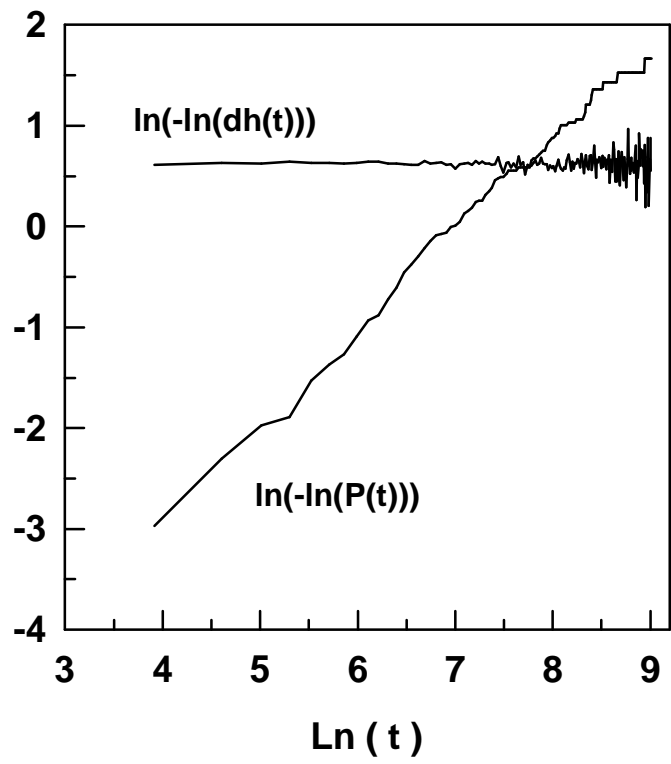


FIGURE 4

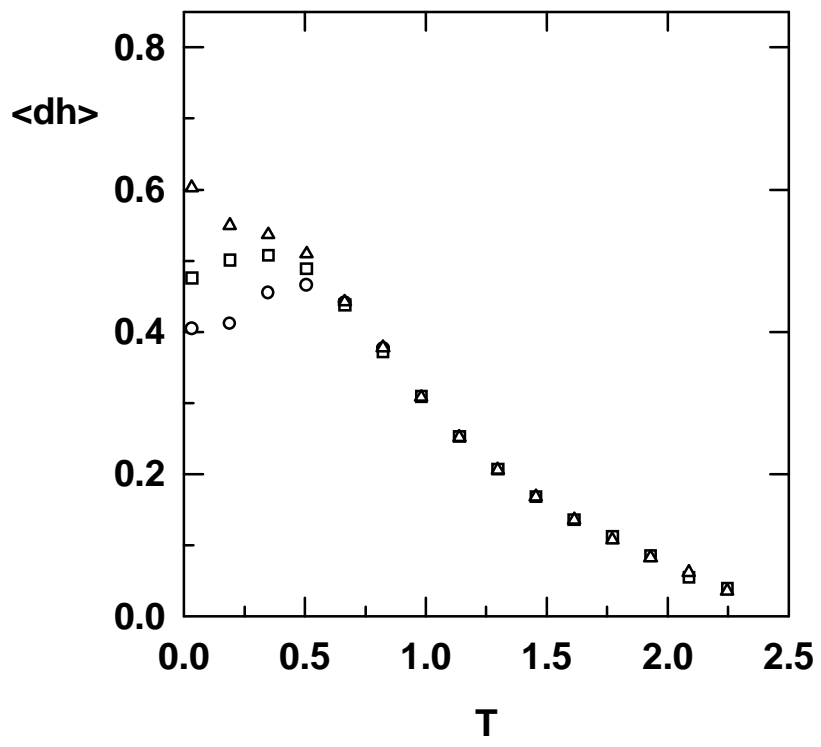


FIGURE 5

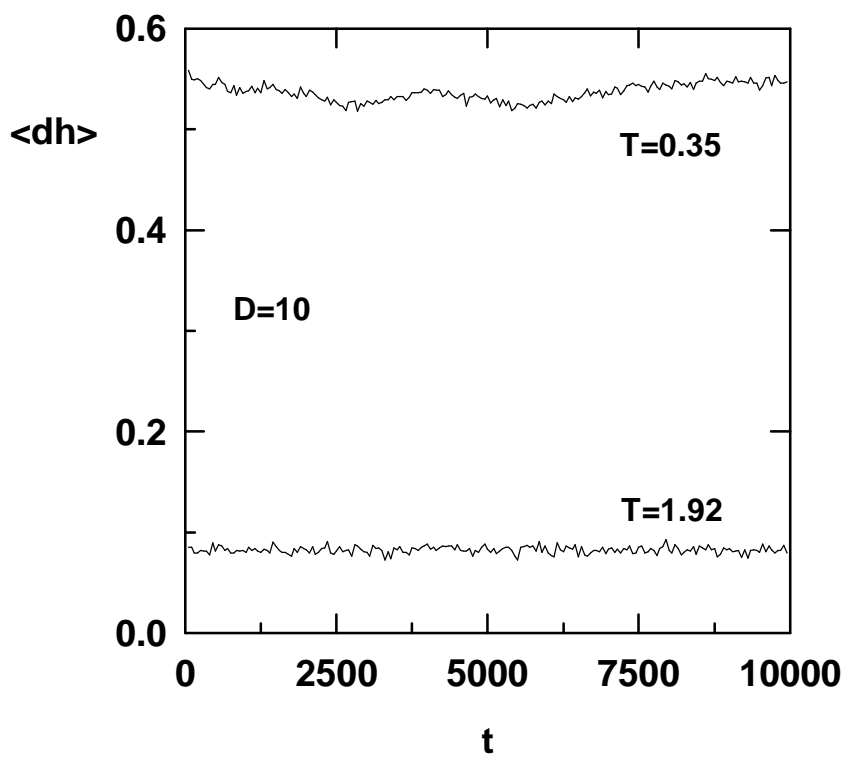


FIGURE 6

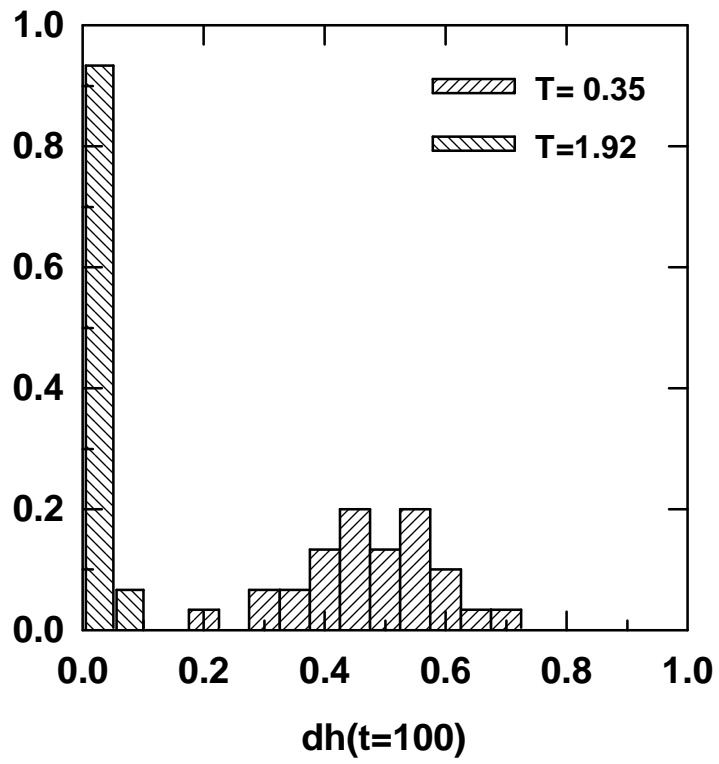


FIGURE 7

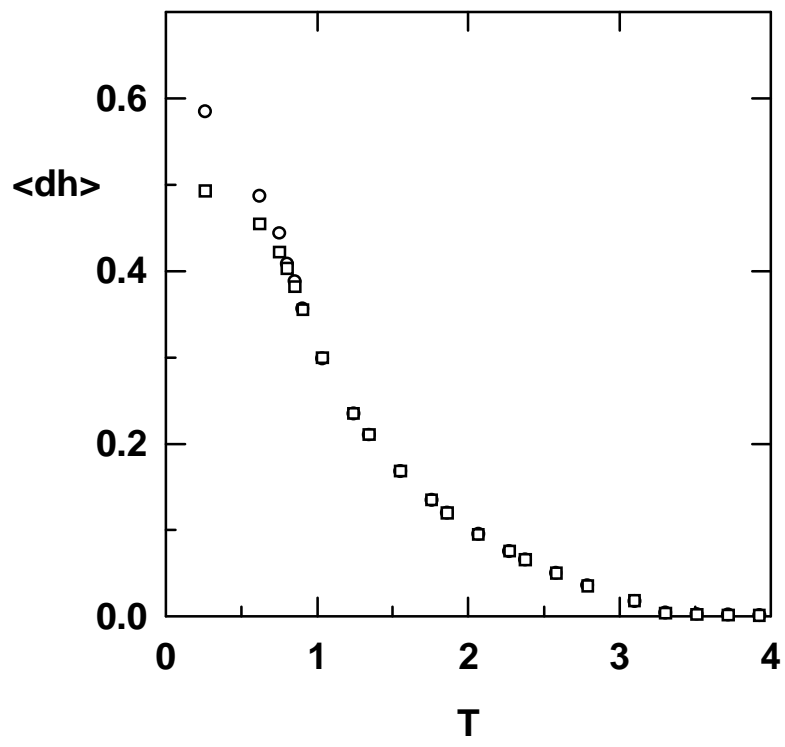


FIGURE 8